Interference Gaussianization: Time-Domain Inter-Symbol Spreading for Blind Adaptive Array Signal Source Identification

KAZUKI MARUTA[1], (Member, IEEE), **KATSUYA SENOO**[2], (Graduate Student Member, IEEE),
DAISUKE HISANO[3], (Member, IEEE), **YU NAKAYAMA**[4], (Member, IEEE),
AND KENTARO NISHIMORI[5], (Member, IEEE)

[1]Academy for Super Smart Society, Tokyo Institute of Technology, Tokyo 152-8552, Japan
[2]Graduate School of Engineering, Chiba University, Chiba 263-8522, Japan
[3]Graduate School of Engineering, Osaka University, Osaka 565-0871, Japan
[4]Institute of Engineering, Tokyo University of Agriculture and Technology, Tokyo 184-8588, Japan
[5]Faculty of Engineering, Niigata University, Niigata 950-2181, Japan

Corresponding author: Kazuki Maruta (kazuki.maruta@ieee.org)

ABSTRACT This paper proposes a novel blind adaptive array (BAA) interference suppression scheme incorporated with a time-domain symbol spreading (TISS). It can expand an operational region of BAA irrespective of input signal-to-interference power ratio (SIR) conditions. Independent component analysis (ICA) and constant modulus algorithm (CMA) are expected as the promising BAA approaches to suppress unknown interference which is extensively caused due to the small cell densification and spectrum superposing between a plurality of wireless communication systems. These BAA algorithms basically require an input SIR to be larger than 0 dB to suppress interference by capturing the desired signal appropriately. The proposed scheme applies TISS to the transmission signal for the desired user and then de-spreads it at the receiver side. It Gaussianizes statistical inherence of the interference signals and can bring beneficial effects; reducing the kurtosis for ICA as well as collapsing the constant envelope properties for CMA. Such intentional modification to the interference signals can improve the capture performance of the desired signal and realize its effective identification even at SIR < 0 dB. Its fundamental effectiveness is presented through various perspectives such as input SIR, symbol amount, and modulation orders.

INDEX TERMS Adaptive arrays, blind source separation, independent component analysis, constant modulus algorithm, Gaussianization, time-domain inter-symbol spreading.

I. INTRODUCTION

Due to the rapid widespread of various mobile communication systems and the growth of user demands, exploding mobile traffic should be dealt with efficiently. Small cell densification is now seen to be a straightforward means to enhance the areal system capacity [1], [2]. It can alleviate traffic load to be supported by a per base station (BS) or access point (AP) without enlarging the transmission bandwidth. Especially, the microwave band faces severe spectrum resource exhaustion. It forces BSs to be deployed in

a single frequency reuse manner. Under such constraint, inter-cell interference (ICI) dominates the system capacity and thus dense BS deployment may conversely cause capacity degradation.

The concept of effective use of spectrum resources is extended to sharing among a plurality of systems so-called cognitive radio [3], [4]. Under the constraint so as not to interfere with the existing (i.e. primary) system, secondary systems detect available radio resources for their communication. A recent practical trend is to build a database [5], [6] which records statistical usage of spectrum resources such as signal intensities with corresponding measurement points [7] and secondary users can refer to it to dynamically access

temporarily unused spectrum. It is premised on conservative use, and the secondary system must communicate under stringent power constraints. Further, such a white space-filling approach cannot substantially enhance the spectral efficiency beyond 100%. A more aggressive approach is investigated to fully exploit an unlicensed spectrum. Its fundamental concept was discussed as a licensed assisted access (LAA) [8] and new radio-based access to unlicensed spectrum (NR-U) [9], [10]. It aims a coexistence of cellular systems and wireless LANs in an unlicensed band originally resided by the latter ones. Although these systems should avoid the co-channel inter-system interference in a distributed manner known to listen before talk (LBT) mechanism, it has basically arisen from the time-division principle; overall spectral efficiency cannot be improved as well.

A. SPECTRUM SUPERPOSING

Spectrum superposing [11], [12], sharing the spectral resources in a spatial domain, is believed to one of the promising conceptions to drastically enhance the spectral efficiency. It can provide an open wireless environment where mobile users will be able to enjoy more comfortable communication without legal restrictions. Generally, spatially multiplexed signals can be separated under the knowledge of channel state information (CSI). CSI-aided pre/post coding is specialized for an *intra*-system interference suppression. *Inter*-system interference suppression, however, is quite difficult since the pilot sequence cannot be preshared and the signal format basically differs depending on systems; CSI cannot be obtained. We focused on blind adaptive array (BAA) or blind source separation (BSS) which are well known and effective approaches to suppress unknown interference signals without any a priori information such as CSI. It derives the array weight via the received data signal in an unsupervised manner. However, the target signal to be suppressed is dependent on its derivation principle. Besides, the receiver does not know which of the incoming signals is the desired one or interference. The major challenge in the spectrum superposing is to simultaneously resolve the above problems; our interest is to control the weight derivation process to appropriately suppress the interference using implicit knowledge. The following part reviews various BAA algorithms along with their weight optimization criteria and exposes the key point of our proposal in this paper.

B. RELATED WORK

There exist lots of BAA algorithms with a variety of optimization criteria. Maximal ratio combining (MRC) aligns the phase component of the received signal so as to extract the dominant signal [13], i.e. having the largest signal power. Power inversion (PI), as the name implies, reverses the power ratio relationship of the received signal [14]. Eigenvector beamspace weighting can derive respective beams to strengthen the power of incoming signals [15]. Constant modulus algorithm (CMA) exploits the constant envelope property of the modulated signal [16], [17]. It suppresses

interference by optimizing the signal amplitude distorted by interference to be constant. Independent component analysis (ICA), which is originally investigated for acoustic/speech signal source separation [18], [19], is also widely applied to wireless field such as blind spatial multiplexing [20]–[22]. Its optimization criterion is based on *kurtosis* or *negentropy* which express a non-Gaussian property. Among them, CMA and ICA have strong interference suppression capability [23].

Other algorithms are being developed actively for BSS with exploiting the non-Gaussian property of signal sources [24]. For spatially correlated signals, sparse component analysis (SCA) is considered a challenging method [25]. This idea is close to compressed sensing, which has recently been widely applied to the direction of arrival estimation [26], [27]. Although it can alleviate an assumption on statistical independence of signal sources generally required for other approaches, its computational simplification is the main object of interest [28]. Further, the geometric inherence is also available as the deterministic properties of the transmitted signals, named boundary component analysis (BCA) [29], [30]. It is claimed that signal separation is possible with fewer symbols because the BCA does not use statistical information. However, the above approaches have not validated their effectiveness against the intensity of the interference signal, which is an important measure for considering the spectrum superposing scenario. The conventional idea is to adaptively switch different algorithms upon the understanding of signal-to-interference power ratio (SIR) conditions. Since the SIR is also unknown, its blind estimation before the interference suppression is also a major challenge [31]. In addition to that, the above mentioned blind approaches require to identify the desired signals after the separation due to their blind nature. Unique words should be inserted into each spatial signal stream for that purpose and thus eventually causes an overhead.

C. CONTRIBUTION OF THIS WORK

The various approaches described above use the inherent properties of signal sources as a weight derivation principle and attempt to separate them. Key idea of our proposal is to improve the signal source separation capability by deliberately modifying its nature, which is higher-order statistics in this paper. Suppose a synchronized transmission such as uplink multiple access (MA) channel for the intra-system, all incoming signals have the same statistical inherence which weakens the signal identification ability of ICA and CMA. In this case, ICA or CMA attempts to capture the signal having the dominant component, i.e. the largest signal power. It indicates that the SIR at the antenna input should be larger than 0 dB; it is the BAA requirement at the initial state. Our approach attempts to eliminate such a limitation, that is, to obtain the desired signal without fail irrespective of interference conditions. It has not been considered so far.

This paper proposes a time-domain inter-symbol spreading (TISS) for BAA in the synchronous interference suppression scenario. A spreading matrix is multiplied to the
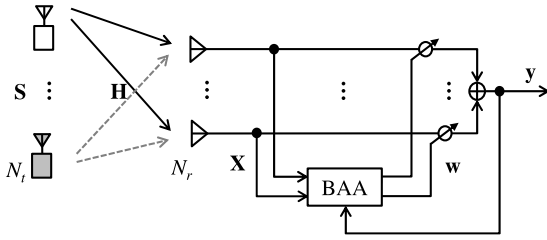
FIGURE 1. System model.

desired transmission symbol sequences and de-spreading is performed to the received signal which is the mixture of desired and interference signals. It intentionally modifies the statistical inherence of interference signals to follow the Gaussian distribution without signal bandwidth enlargement. ICA and CMA can well capture the desired signal irrespective of the input SIR and thus interference can be successfully suppressed. It can also realize the signal identification without any additional unique words since the spreading matrix takes responsibility for that. From another perspective, BAA interference suppression capability is generally weakened in higher-order quadrature amplitude modulation (QAM) since the signal statistics retrogress to Gaussian. Higher datarate transmission is quite essential in the recent wireless communication and hence the spectrum superposing should also be attained even in higher-order such as 1024QAM, for more efficient spectrum resource utilization. The proposed scheme can maintain improved interference suppression capability under such various modulation conditions.

The main contribution of this paper is to present a novel interference suppression scheme by applying its Gaussianization which can expand the operational region of BAAs such as SIR and QAM order. Its fundamental effectiveness is disclosed through a computer simulation. The rest of this paper is organized as follows. Section II and Section III describe system model and BAA algorithms of interest, respectively. Section IV presents the proposed scheme. Section V then shows the interference suppression performance provided by our proposal through computer simulations. Section VI concludes this paper.

II. SYSTEM MODEL

Throughout the paper, normal letters represent scalar quantities, bold lowercase letters indicate vectors and uppercase letters indicate matrices. $|.|$, $(.)^T$, $(.)^H$ and $E(.)$ indicate absolute values, transpose, conjugate transpose and expectation (ensemble averaging), respectively. Let N_t, N_r and N_s denote the number of transmitters, receiving antenna elements and modulated data symbols. Transmitter is assumed to have one antenna. Fig. 1 depicts a system model of interest. Suppose a narrow band single-carrier transmission, $\mathbf{s}_i \in \mathbb{C}^{1 \times N_s}$, $\mathbf{X} \in \mathbb{C}^{N_r \times N_s}$ and $\mathbf{H} \in \mathbb{C}^{N_r \times N_t}$ denote the transmission signal from the i-th ($i = 1, 2, \ldots, N_t$) transmitter, the array input at the receiver side, and the channel matrix, respectively. Based on the spatial multiplexing conception, these relationship can be

mathematically expressed as follows [23], [32].

$$\mathbf{X} = \mathbf{HGS} + \mathbf{N}, \tag{1}$$

$$\mathbf{S} = \begin{pmatrix} \mathbf{s}_1 \\ \vdots \\ \mathbf{s}_i \\ \vdots \\ \mathbf{s}_{N_t} \end{pmatrix} = \begin{pmatrix} s_{1,1} & \cdots & s_{1,k} & \cdots & s_{1,N_s} \\ \vdots & \ddots & & & \vdots \\ s_{i,1} & & s_{i,k} & & s_{i,N_s} \\ \vdots & & & \ddots & \vdots \\ s_{N_t,1} & \cdots & s_{N_t,k} & \cdots & s_{N_t,N_s} \end{pmatrix}, \tag{2}$$

$$\mathbf{H} = \begin{pmatrix} \mathbf{h}_1 & \cdots & \mathbf{h}_i & \cdots & \mathbf{h}_{N_t} \end{pmatrix}$$
$$= \begin{pmatrix} h_{1,1} & \cdots & h_{1,i} & \cdots & h_{1,N_t} \\ h_{2,1} & & h_{2,i} & & h_{2,N_t} \\ \vdots & & \vdots & \ddots & \vdots \\ h_{N_r,1} & \cdots & h_{N_r,i} & \cdots & h_{N_r,N_t} \end{pmatrix}, \tag{3}$$

$$\mathbf{G} = \begin{pmatrix} g_1 & 0 & \cdots & 0 \\ 0 & g_2 & & \vdots \\ \vdots & & \ddots & 0 \\ 0 & \cdots & 0 & g_{N_t} \end{pmatrix}, \tag{4}$$

where the diagonal matrix, $\mathbf{G} \in \mathbb{C}^{N_t \times N_t}$, provides a strength for each transmission signal. $\mathbf{N} \in \mathbb{C}^{N_r \times N_s}$ denotes the additive white Gaussian noise (AWGN) each element of which follows $\mathcal{CN}(0, \sigma^2)$. Note the transmission symbols, $\mathbf{s}_i$, is a row vector, and the channel vector, $\mathbf{h}_i$, that $\mathbf{s}_i$ experiences is a column vector. BAA weight, $\mathbf{w} = (w_1, w_2, \ldots, w_{N_r})^T \in \mathbb{C}^{N_r \times 1}$, is then derived by respective algorithms to be presented later, and is multiplied to the received signal, $\mathbf{X}$, to obtain the array output, $\mathbf{y} \in \mathbb{C}^{1 \times N_s}$:

$$\mathbf{y} = \mathbf{w}^H \mathbf{X}$$
$$= \begin{pmatrix} y_1 & \cdots & y_k & \cdots & y_{N_s} \end{pmatrix}. \tag{5}$$

As mentioned in the Section I-C, the array output is not always the desired signal. It conventionally depends on the conditions of the interference level. It is the key challenge of the completely blind interference suppression, that is, how to derive an optimal weight so as to obtain the desired signal regardless of the interference condition.

III. BLIND ADAPTIVE ARRAY ALGORITHMS
A. INDEPENDENT COMPONENT ANALYSIS (ICA)
ICA generally utilizes a non-Gaussian inherence of signal sources known to *kurtosis* or *negentropy*. This study mainly focuses on kurtosis representing the higher order signal statistics. The kurtosis of complex random variables can be defined as follows [33],

$$\mathcal{K}(\mathbf{w}_{\text{ICA}}(m))$$
$$= \frac{\frac{1}{N_s}\sum_{k=1}^{N_s}|y_k|^4 - 2\left(\frac{1}{N_s}\sum_{k=1}^{N_s}|y_k|^2\right)^2 - \left|\frac{1}{N_s}\sum_{k=1}^{N_s}y_k^2\right|^2}{\left(\frac{1}{N_s}\sum_{k=1}^{N_s}|y_k|^2\right)^2}$$
$$= \frac{N_s(\mathbf{y}\odot\mathbf{y})(\mathbf{y}\odot\mathbf{y})^H - 2\left(\mathbf{y}\mathbf{y}^H\right)^2 - \left|\mathbf{y}\mathbf{y}^T\right|^2}{\left(\mathbf{y}\mathbf{y}^H\right)^2}. \tag{6}$$

⊙ indicates the Hadamard product, i.e. element-wise multiplication. Kurtosis often represents *tailedness* and *peakedness* of the random variables distribution. Its recent interpretation is understood as *tailedness* rather than *peakedness* [34]. When the complex random variables have a non-Gaussian inherence, the value of kurtosis goes negative. The kurtosis value of zero, on the contrary, indicates that the signal has a completely Gaussian distribution. Through various kinds of algorithms for ICA have been conceived, they generally require preprocessing known as *centering* and *whitening*. Meanwhile, RobustICA, eliminating the above preprocessing with a straightforward steepest descent approach, has been developed [19]. It also necessitates searching the optimal step size, $\mu_{opt} \in \mathbb{R}^1$, for each iteration stage so that the kurtosis can be minimized. RobustICA can exhibit superior convergence for weight derivation as well as stable interference suppression capabilities better than other ICA derivatives such as FastICA [23]. We treat RobustICA attracted its possibility and aims to improve its blind interference suppression performance.

The following steps attain BAA weight derivation on RobustICA [19];

$$\mathbf{y} = \mathbf{w}_{ICA}^H(m)\,\mathbf{X}, \tag{7}$$

$$\mathbf{e}_{ICA} = \frac{4}{\left(\mathbf{yy}^H\right)^2}\left[N_s\mathbf{yy}^H\left(\mathbf{Xy}^T\right) - \mathbf{X}\left(\mathbf{y}\odot\mathbf{y}\odot\mathbf{y}^*\right)\right.$$

$$\left. - \frac{\left\{N_s\left(\mathbf{y}\odot\mathbf{y}\right)\left(\mathbf{y}\odot\mathbf{y}\right)^H - \left|\mathbf{yy}^T\right|^2\right\}\mathbf{Xy}^H}{\mathbf{yy}^H}\right], \tag{8}$$

$$\mu_{opt} = \arg\min_{\mu}\left(\mathcal{K}(\mathbf{w}_{ICA}(m) - \mu\mathbf{e}_{ICA})\right), \tag{9}$$

$$\mathbf{w}_{ICA}(m+1)$$
$$= \mathbf{w}_{ICA}(m) - \mu_{opt}\mathbf{e}_{ICA}. \tag{10}$$

$\mathbf{e}_{ICA} \in \mathbb{C}^{N_r \times 1}$ in (8) is the error component to update the weight vector. The value of kurtosis is uniquely determined for respective QAM order since the possible distribution of complex signals is dependent on them.

B. CONSTANT MODULUS ALGORITHM (CMA)

Array weight derivation principle of CMA is to optimize the amplitude of array output, $\mathbf{y}$, so as to have the constant envelope, i.e. to minimize the following cost function;

$$Q(\mathbf{w}_{CMA}(m)) = \frac{1}{N_s}\sum_{k=1}^{N_s}\left||y_k|^p - \delta^p\right|^q$$

$$= \frac{1}{N_s}\sum_{k=1}^{N_s}\left|\left|(\mathbf{w}_{CMA}^H(m)\mathbf{X})_k\right|^p - \delta^p\right|^q. \tag{11}$$

It is a generalized definition [35]. Here, $(\mathbf{a})_k$ indicates the k-th entry of the vector $\mathbf{a}$. δ denotes the constant envelope value and is defined as 1. p and q take values of 1 or 2, respectively, and these settings provides a specific weight derivation criterion. When $p = 1$ and $q = 2$, the weight update manner can be expressed in a special form not including the step size.

It is called least square CMA (LS-CMA) [17] and is known to exhibit a superior convergence characteristics.

$$\mathbf{y} = \mathbf{w}_{CMA}^H(m)\mathbf{X}, \tag{12}$$

$$e_{CMA,k} = \frac{\delta y_k}{|y_k|}, \tag{13}$$

$$\mathbf{w}_{CMA}(m+1)$$
$$= \mathbf{w}_{CMA}(m) - \left(\mathbf{XX}^H\right)^{-1}\mathbf{X}\left(\mathbf{y} - \mathbf{e}_{CMA}\right)^H$$

$$= \mathbf{w}_{CMA}(m) - \left(\mathbf{XX}^H\right)^{-1}\mathbf{X}\left(\mathbf{w}_{CMA}^H(m)\mathbf{X} - \mathbf{e}_{CMA}\right)^H$$

$$= \mathbf{w}_{CMA}(m) - \left(\mathbf{XX}^H\right)^{-1}\left(\mathbf{XX}^H\mathbf{w}_{CMA}(m) - \mathbf{Xe}_{CMA}^H\right)$$

$$= \left(\mathbf{XX}^H\right)^{-1}\mathbf{Xe}_{CMA}^H. \tag{14}$$

$\mathbf{e}_{CMA} \in \mathbb{C}^{1 \times N_s}$ in (13) is the error vector and the amplitudes of those elements are normalized to the constant envelope value. The above formulation is similar to the minimum mean square error (MMSE) criteria based on a sample matrix inversion (SMI) [36]. The normalized array output, $\delta y_k/|y_k|$, in (14) can be regarded as the reference symbol in the MMSE-SMI. Although the CMA is known to work under the use of multi modulus signal such as 16QAM [37], it cannot avoid the degradation of interference suppression capability due to the nature of its optimization criterion, as the number of envelopes increases.

IV. PROPOSED SCHEME

Suppose the synchronized transmission scenario such as intra-system MA channel, the desired and interference signals have almost the same property which limits the blind interference suppression capabilities of ICA and CMA. In this case, both BAA algorithms capture the signal which dominates the mixture of the desired and interference components, i.e. the larger signal strength. Therefore, its operational region is limited to SIR > 0 dB. The signals' property indicates the kurtosis for ICA and the constancy for CMA. The kurtosis, κ, takes the minimum value of -2.0 for BPSK and that for $M \geq 4$ is derived as [33],

$$\kappa = -\frac{3}{5}\frac{M+1}{M-1}. \tag{15}$$

It tends to decrease for the higher modulation order and converges on -0.60. As for the CMA, the possible number of constant envelopes (moduli), η, for $M \geq 4$ can be counted from the isosceles right triangle part of a quadrant of the IQ constellation;

$$\eta = \frac{1}{2}\frac{\sqrt{M}}{2}\left(\frac{\sqrt{M}}{2} + 1\right)$$

$$= \frac{1}{8}\sqrt{M}\left(\sqrt{M} + 2\right). \tag{16}$$

It increases in proportion to the modulation order and diverges as $M \to \infty$. These concrete values for each modulation order are summarized in Table 1. Both kurtosis and moduli increase as the modulation order is raised. Since these
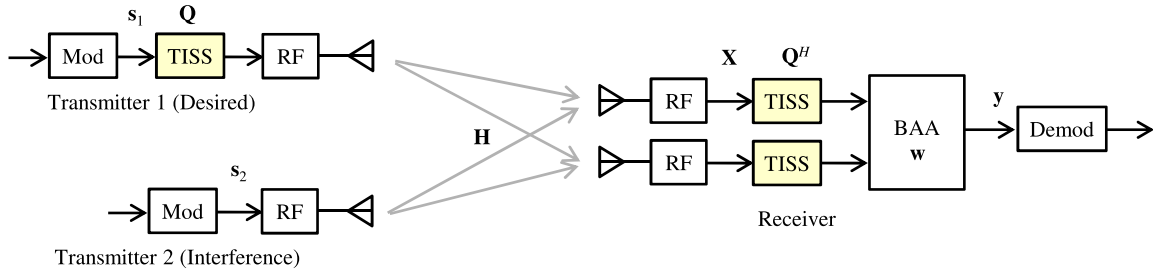
FIGURE 2. Proposed structure of the transmitter and receiver.

TABLE 1. Signal properties for modulation orders.

Modulation order M	Kurtosis κ	Moduli η
2	−2.0000	1
4	−1.0000	1
16	−0.6800	3
64	−0.6190	10
256	−0.6047	36
1024	−0.6012	136
∞	−0.6000	∞
(i.i.d)	0	∞

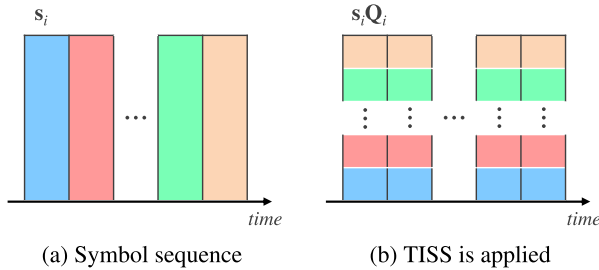(a) Symbol sequence   (b) TISS is applied

FIGURE 3. Concept of time-domain inter-symbol spreading.

metrics have a noticeable difference compared to the case of i.i.d, i.e. $\kappa = 0$ for ICA and $\eta = \infty$ for CMA, we can expect that these tendencies are available for signal separation. In particular for ICA, the κ approaches to -0.6 at $M \to \infty$, which is obviously different from the $\kappa = 0$ in the i.i.d case. ICA optimizes the array weight so as to minimize the kurtosis as defined in (9). Therefore ICA can effectively suppress interference signals having normal distribution even for higher modulation order such as 1024QAM.

Exploiting the above feature, the proposed scheme intentionally Gaussianizes the statistical inherence of the time-domain symbol sequence by the inter-symbol spreading operation. A schematic structure of the transmitter and receiver for the proposed scheme is drawn in Fig. 2. A specified spreading matrix, $\mathbf{Q}_i \in \mathbb{C}^{N_s \times N_s}$, is shared between the i-th transmitter and receiver in advance. The proposed transmitter firstly multiplies the transmission symbol sequence by this spreading matrix.

$$\mathbf{s}_i \leftarrow \mathbf{s}_i \mathbf{Q}_i. \tag{17}$$

This operation can be intuitively visualized as shown in Fig. 3. Let $\mathbf{I}_{N_s} \in \mathbb{C}^{N_s \times N_s}$ and $\mathbf{U} \in \mathbb{C}^{N_s \times N_s}$ denote the identity and arbitrary non-zero matrices, the spreading matrix, $\mathbf{Q}_i$, is defined so as to hold the following condition.

$$\mathbf{Q}_i \mathbf{Q}_j^H = \begin{cases} \mathbf{I}_{N_s} & (i = j) \\ \mathbf{U} & (i \neq j). \end{cases} \tag{18}$$

The spreading matrix can be arbitrarily chosen as long as the above constraint is satisfied.[1] A simple matrix inversion operation is also acceptable. This study employs an unitary matrix to avoid the undesirable impact to the additive noise term. In this case, $\mathbf{U}$ is also the unitary.

$\mathbf{Q}_i$ can also be constructed by arranging the partial spreading matrix, $\mathbf{P}_i \in \mathbb{C}^{N_q \times N_q}$ ($N_q \leq N_s$), in a diagonal manner;

$$\mathbf{Q}_i = \begin{pmatrix} \mathbf{P}_i & 0 & \cdots & 0 \\ 0 & \mathbf{P}_i & & \vdots \\ \vdots & & \ddots & 0 \\ 0 & \cdots & 0 & \mathbf{P}_i \end{pmatrix}. \tag{19}$$

$$\text{s.t. } N_q \mid N_s, \tag{20}$$

Here we define N_q as the spreading factor and the notation $. \mid .$ indicates that the integer N_q is a divisor of the integer N_s. Other interfering transmitters ($j \neq i$) do not apply the TISS, or prepare other different spreading matrices. The desired/interference signals are then transmitted and arrived at the receiver through the propagation channels. The received signal is expressed as follows,

$$\mathbf{X} = \mathbf{h}_i \mathbf{s}_i \mathbf{Q}_i + \sum_{j \neq i}^{N_t} \mathbf{h}_j \mathbf{s}_j \mathbf{Q}_j + \mathbf{N}$$

$$= \begin{pmatrix} h_{1,i} \\ \vdots \\ h_{N_r,i} \end{pmatrix} \mathbf{s}_i \mathbf{Q}_i + \sum_{j \neq i}^{N_t} \begin{pmatrix} h_{1,j} \\ \vdots \\ h_{N_r,j} \end{pmatrix} \mathbf{s}_j \mathbf{Q}_j + \mathbf{N}. \tag{21}$$

---

[1] $\mathbf{Q}_i \mathbf{Q}_j^H = \mathbf{U}$ ($i \neq j$) may possibly have special properties close to the identity matrix. More specifically, consider $\mathbf{Q}_1 \mathbf{R}_1 = \mathbf{A}$ and $\mathbf{Q}_2 \mathbf{R}_2 = \mathbf{B}$, the requirement in (18) will be broken if each element of randomly prepared $\mathbf{A}$ and $\mathbf{B}$ has very close values. Practically, for instance, we can prepare matrices $\mathbf{Q}_i$ ($i = 1, 2, \ldots, N_t$) and assign them to transmitters such that the matrix product of any combination among them has an arbitrary value.

Algorithm 1 Proposed BAA With TISS

Transmitter:
1: Set random complex matrix: $\mathbf{A}_i$
2: QR decomposition: $\mathbf{Q}_i \mathbf{R}_i = \mathbf{A}_i$
3: $\mathbf{s}_i \leftarrow \mathbf{s}_i \mathbf{Q}_i$
Receiver:
4: $\mathbf{X} \leftarrow \mathbf{X} \mathbf{Q}_i^H$
5: $m \leftarrow 0$
6: $\mathbf{w}(m) \leftarrow (1, 0, \dots, 0)$
7: **while** $m < N_{\mathrm{m}}$ **do**
8: $\quad \mathbf{y} \leftarrow \mathbf{w}^H(m+1)\mathbf{X}$
9: $\quad \mathbf{e} \leftarrow \mathcal{F}(\mathbf{y}, \mathbf{X})$
10: $\quad \mathbf{w}(m+1) \leftarrow \mathcal{G}(\mathbf{w}, \mathbf{X}, \mathbf{e}, \mu)$
11: $\quad \mathbf{w}(m+1) \leftarrow \mathbf{w}(m+1)/\|\mathbf{w}(m+1)\|$
12: $\quad m \leftarrow m+1$
13: **end while**

De-spreading is performed by applying the same matrix, $\mathbf{Q}_i^H$, to the received symbol sequences for all antenna elements.

$$\mathbf{X} \leftarrow \mathbf{X} \mathbf{Q}_i^H \tag{22}$$

$$= \mathbf{h}_i \mathbf{s}_i + \sum_{j \neq i}^{N_{\mathrm{t}}} \mathbf{h}_j \mathbf{s}_j \mathbf{Q}_j \mathbf{Q}_i^H + \mathbf{N} \mathbf{Q}_j \mathbf{Q}_i^H. \tag{23}$$

The above operation returns the desired signal to its original sequence whereas the interference signals are de-spread. Suppose unitary spreading matrices, these multiplication is also the unitary and thus effectiveness of our proposal holds irrespective of applying TISS for other transmitters. Then BAA schemes are applied. Its overall procedure for the i-th transmitter/receiver is summarized in Algorithm 1. Here, the function $\mathcal{F}$ calculates the error components as described in (8) and (13). $\mathcal{G}$ indicates the weight update function as described in (10) and (14), respectively. $\|.\|$ stands for the Frobenius (Euclidean) norm.

Fig. 4 exemplifies the two-dimensional histogram (or called probability density function (PDF)) of spread 16QAM symbols at $N_{\mathrm{s}} = 100$. The kurtosis value is increased to -0.0138 from -0.68 by spreading; approaches to the normal (Gaussian) distribution. Independent complex random variables, having properties close to the uniform distribution such as QAM symbols, are replaced with their respective summations. This simple operation leads the complex signal distribution to the Gaussian according to the *central limit theorem* (CLT) [38]. Its classical form claims that a normalized summation of independent random variables with arbitrary distribution tends to have a normal distribution. When $(z_1, \dots, z_N)$ follow independent and identically distributed (i.i.d) random variables with mean ξ and variance ρ^2, these arithmetic average,

$$\bar{z} = \frac{1}{N} \sum_{k=1}^{N} z_k, \tag{24}$$

is also one of the random variables. The distribution of $\bar{z}$ approaches to the normal distribution each with mean ξ and variance ρ^2/N as $N \to \infty$. As for the proposed scheme, it derives the new complex random variables by applying spreading matrix, $\mathbf{Q}_i = \frac{1}{N_{\mathrm{q}}}(q_{i,k,j})$, to the transmission symbol sequence. Focusing on the first N_{q} symbols to which the partial spreading matrix, $\mathbf{P}_i$, is applied, we have

$$\bar{s}_{i,l} = \frac{1}{N_{\mathrm{q}}} \sum_{k=1}^{N_{\mathrm{q}}} s_{i,k} q_{i,k,l}. \tag{25}$$

Multiplication $s_{i,k} q_{i,k,l}$ are random variables and thus these summation over N_{q} symbols also follows the normal distribution. Based on the proof of CLT in [38, pp. 36–38], it can be derived as follows. First, each multiplication $s_{i,k} q_{i,k,l}$ is rewritten as,

$$s'_k := s_{i,k} q_{i,k,l}. \tag{26}$$

It is also a random variable having an arbitrary distribution with mean ξ and variance ρ^2. Here we justify the new random variable in (25), key feature of the proposed TISS, could follow the normal distribution. We exploit properties of the first and second characteristic functions which are defined [39, p. 41],

$$\Phi_{s'_k}(t) := E\left[\exp\left(\mathrm{j}t s'_k\right)\right], \tag{27}$$

$$\Gamma_{s'_k}(t) := \ln \Phi_{s'_k}(t) = \sum_{m=0}^{\infty} \kappa_m \frac{(\mathrm{j}t)^m}{m!}, \tag{28}$$

where $t \in \mathbb{R}$ is an arbitrary index. The second characteristic function in (28) is given by the logarithm of the first one and its Taylor series expansion. It is also called the cumulant generating function; coefficient κ_m yields the m-th cumulant and is obtained as,

$$\kappa_m = \left. \frac{d^m \Gamma_{s'_k}(t)}{d(\mathrm{j}t)^m} \right|_{t=0}. \tag{29}$$

Note that $\Gamma_{s'_k}(0) = 1$, $\Gamma_{s'_k}^{(m)}(0) = E[s'^m_k]$ (for $m = 1, 2, \dots$), at $t = 0$, the first three cumulates can be obtained as,

$$\kappa_0 = 0, \tag{30}$$

$$\kappa_1 = E[s'_k] = \xi, \tag{31}$$

$$\kappa_2 = E[s'^2_k] - E[s'_k]^2 = \rho^2. \tag{32}$$

We then attempt to derive that the first characteristic function of the new random variables applied TISS in (25),

$$\Phi_{\bar{s}_l}(\tau) = E\left[\exp(\mathrm{j}\tau \bar{s}_l)\right], \tag{33}$$

converges to that of the normal distribution with $\mathcal{CN}$ $(\xi, \rho^2/N_{\mathrm{q}})$ [40, p. 238], i.e.

$$\Phi_{\mathrm{norm}}(\tau) \approx \exp\left(\mathrm{j}\tau \xi - \frac{\tau^2(\rho^2/N_{\mathrm{q}})}{2}\right), \tag{34}$$

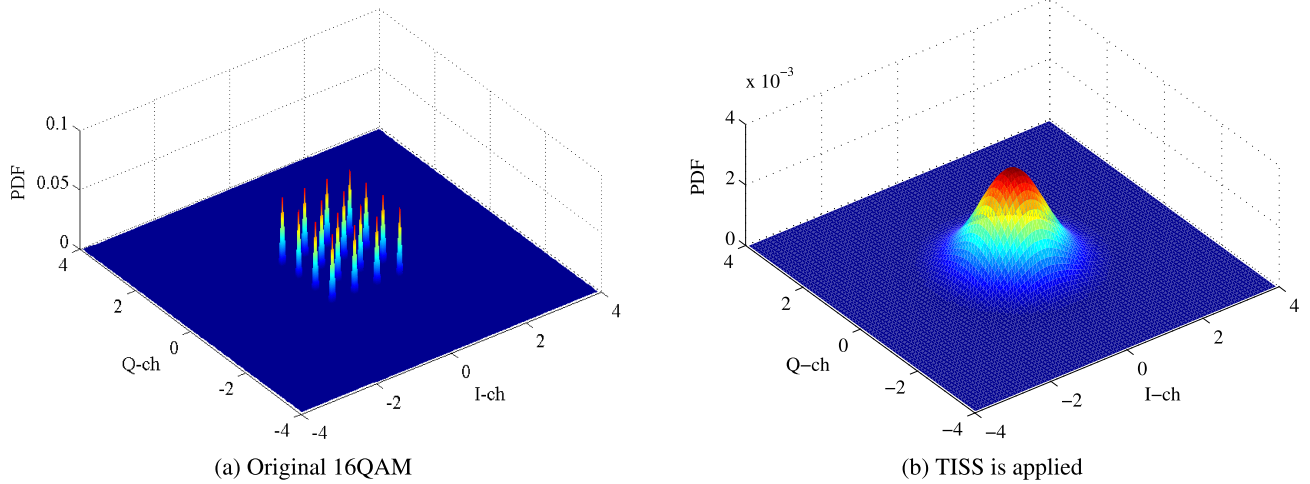under $N_{\mathrm{q}} \to \infty$.

(a) Original 16QAM

(b) TISS is applied

FIGURE 4. Two-dimensional histogram for 16QAM ($N_s = N_q = 100$).

(33) can be rewritten by using (25) and (27) as,

$$\Phi_{\bar{s}_l}(\tau) = E\left[\exp(j\tau \bar{s}_l)\right]$$

$$= E\left[\exp\left(j\tau \frac{1}{N_q}\sum_{k=1}^{N_q} s'_k\right)\right]$$

$$= E\left[\prod_{k=1}^{N_q}\exp\left(j\frac{\tau}{N_q}s'_k\right)\right]$$

$$= \prod_{k=1}^{N_q} E\left[\exp\left(j\frac{\tau}{N_q}s'_k\right)\right]$$

$$= \prod_{k=1}^{N_q}\Phi_{s'_k}\left(\frac{\tau}{N_q}\right), \qquad (35)$$

where following general properties are used;

$$\exp\left(\sum_{k=1}^{N_q} z_k\right) = \prod_{k=1}^{N_q}\exp\left(z_k\right), \qquad (36)$$

$$E[\zeta z] = E[\zeta]E[z]. \qquad (37)$$

Since each variable, s'_k, is independent and follows the same distribution for arbitrary k, the above characteristic functions, $\Phi_{s'_k}(\tau)$, are identical. Therefore (35) is further modified to

$$\Phi_{\bar{s}_l}(\tau) = \left\{\Phi_{s'_k}\left(\frac{\tau}{N_q}\right)\right\}^{N_q}. \qquad (38)$$

$\Phi_{\bar{s}_l}(\tau)$ can be expressed by applying an exponential of the second characteristic function in (28),

$$\Phi_{\bar{s}_l}(\tau)$$

$$= \left\{\Phi_{s'_k}\left(\frac{\tau}{N_q}\right)\right\}^{N_q}$$

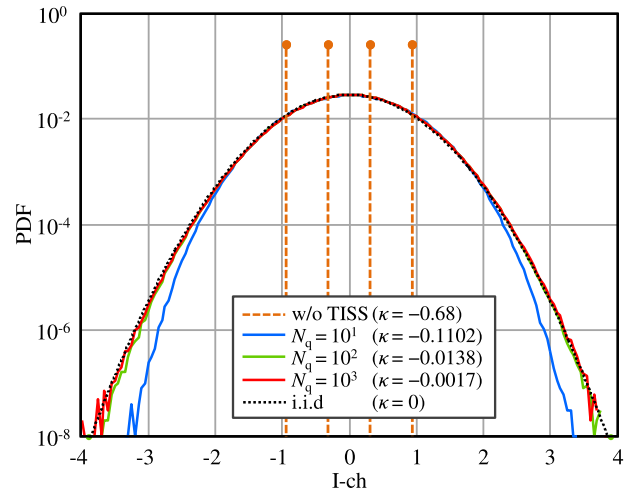$$= \left[\exp\left\{\sum_{m=0}^{\infty}\kappa_m\frac{(j\tau/N_q)^m}{m!}\right\}\right]^{N_q}$$

FIGURE 5. One-dimensional histogram for 16QAM. The brackets in the legend indicate the kurtosis values.

$$= \left[\exp\left\{\kappa_0 + \frac{1}{N_q}j\tau\kappa_1 + \frac{1}{N_q^2}\kappa_2\frac{(j\tau)^2}{2} + \sum_{m=3}^{\infty}\frac{1}{N_q^m}\kappa_m\frac{(j\tau)^m}{m!}\right\}\right]^{N_q}$$

$$= \exp\left\{N_q\kappa_0 + j\tau\kappa_1 + \frac{1}{N_q}\kappa_2\frac{(j\tau)^2}{2} + \sum_{m=3}^{\infty}\frac{1}{N_q^{m-1}}\kappa_m\frac{(j\tau)^m}{m!}\right\}. \qquad (39)$$

Substituting (30)–(32) into (39) yields

$$\Phi_{\bar{s}_l}(\tau) = \exp\left\{j\tau\xi + \frac{\rho^2}{N_q}\frac{(j\tau)^2}{2} + \sum_{m=3}^{\infty}\frac{1}{N_q^{m-1}}\kappa_m\frac{(j\tau)^m}{m!}\right\}. \qquad (40)$$

Suppose the third and subsequent terms become negligible at $N_q \to \infty$, we have the same expression as (34).

Fig. 5 shows one-dimensional PDFs to examine the dependency of the spreading factor, N_q, with 16QAM. Specifically,

the distribution of QAM symbols is uniform in real and imaginary parts, respectively, therefore, TISS output easily follows the normal distribution with not so large value of N_s. Meanwhile, the spreading length affects to a tailedness of the distribution. It contributes to the reduction of the kurtosis value. Figure also shows the kurtosis for each TISS output. It can be confirmed that $N_q = 10$ is sufficient to differentiate the desired and interference signals. Distribution of signal amplitude asymptotically follows Gaussian, i.e. i.i.d having zero kurtosis, when the spreading factor, N_q, is 100 or more. The kurtosis of the QAM signal is at least -0.6 and is obviously different from zero, so that ICA based on kurtosis minimization can fully exploit this feature to capture the desired signal and properly suppress the interfering signal. As for the CMA, TISS is surely effective since the deviation of interference signal amplitude is largely spread. Furthermore, it can also be confirmed that the constant envelope property is certainly broken. The above principle brings the expectation that the BAA weight derivation by ICA and CMA can appropriately work to suppress interference signals, irrespective of the initial SIR condition.

It should be noted that the proposed TISS cannot expand transmission bandwidth unlike code division multiple access (CDMA). In CDMA, a transmission symbol is combined by the orthogonal spreading code with higher rate. Therefore, the transmission bandwidth is spread in the frequency-domain. The proposed TISS performs spreading operation by inter-symbol superposition as depicted in Fig. 3, so that the signal bandwidth is maintained; there is no spectral efficiency degradation. It is applicable to an orthogonal frequency division multiplexing (OFDM) which is a great majority of current wireless communication systems. Meanwhile the above mentioned principle for the proposed concept is considered to be consistent under the CDMA as the same manner. Although the joint application of CMA and CDMA was studied in literature [41]–[43], they have not yet provided discussions on its interference suppression mechanism.

V. NUMERICAL RESULTS
A. SIMULATION PARAMETERS
Two kinds of signal sources exist; the one is the desired signal and the others are the interference. This study assumes a simplified channel model based on the plane wave approximation [44], [45]. Each coefficient of the channel matrix in (3) is determined by the angle of arrival (AoA), θ, for rigorous evaluation under fixed SIR conditions. It becomes,

$$\mathbf{H} = \begin{pmatrix} 1 & \cdots & 1 \\ e^{-j\frac{2\pi}{\lambda}d\cos\theta_1} & \cdots & e^{-j\frac{2\pi}{\lambda}d\cos\theta_{N_t}} \\ \vdots & & \vdots \\ e^{-j\frac{2\pi}{\lambda}(N_r-1)d\cos\theta_1} & \cdots & e^{-j\frac{2\pi}{\lambda}(N_r-1)d\cos\theta_{N_t}} \end{pmatrix}. \quad (41)$$

AoAs for respective signals are determined at random within the range from $-90°$ to $90°$ with $0.01°$ resolution. Interference suppression performances for above mentioned two BAA algorithms, RobustICA and LS-CMA, are mainly

TABLE 2. Simulation parameters.

Parameters	Values
Number of Transmitter and Receiver antenna elements (N_t, N_r)	$(2, 2), (4, 16)$
Inter-element spacing	Half wavelength
SNR per antenna element	30 dB
Angle of arrival	$-90\ldots90$ degrees
BAA algorithm	RobustICA, LS-CMA, BCA
BAA iteration N_m	100 for RobustICA, LS-CMA 200 for BCA

discussed. Additionally, characteristics of BCA [29] and pilot-aided MMSE [36] algorithms are compared as benchmarks. The maximum iteration count for them is set to 100, which shows sufficient convergence characteristics. As for the RobustICA, the search range for its step size is from -10 to 10; 0.0005 step in the region $|\mu| \le 0.5$, 0.01 step in $0.6 \le |\mu| \le 3$ and 1 step in $4 \le |\mu| \le 10$. The spreading matrix, $\mathbf{Q}_i$, is generated from QR decomposition of an arbitrary regular complex matrix. Under the above condition, output signal-to-interference plus noise power ratio (SINR) is examined in terms of input SIR, the number of symbols, N_s, and the modulation orders. When the desired signal is assumed to be from the 1st transmitter, its array output SINR is defined as,

$$\text{SINR} = \frac{\left|\left(\mathbf{w}^H\mathbf{h}_1\right)\right|^2}{\sum_{j=2}^{N_t}\left|\left(\mathbf{w}^H\mathbf{h}_j\right)\right|^2 + \sigma^2}. \quad (42)$$

Interference-limited condition is supposed in order to clearly discuss the interference suppression capability; signal-to-noise power ratio (SNR) is set to 30 dB. Detailed parameters are listed in Table 2. Unless otherwise specified, we assume $N_q = N_s$.

B. RESULTS: 2 × 2 CASE
First, we observe the case where the number of transmitters and receiver antenna elements are two, i.e. $N_t = N_r = 2$. Fig. 6 shows cumulative distribution functions (CDFs) of array output SINR in the case with 16QAM, $N_s = 100$, input SIR $= -10$ dB. Here we plot characteristics of TISS applied to RobustICA, LS-CMA and BCA as well as that without BAA. The result of MMSE is also disclosed as an optimal performance supported by the known pilot symbols. The conventional schemes without TISS frequently miscapture the interference signal and suppress the desired one; output SINR distribution is impractically degraded. The proposed schemes with TISS successfully work to suppress the interference signal even at SIR $= -10$ dB. BAA well captured the desired signal by spreading the interference signal. Although the interference suppression performance of BCA can be improved by applying TISS, its achievable output SINR is less than that for CMA and ICA. Weight optimization
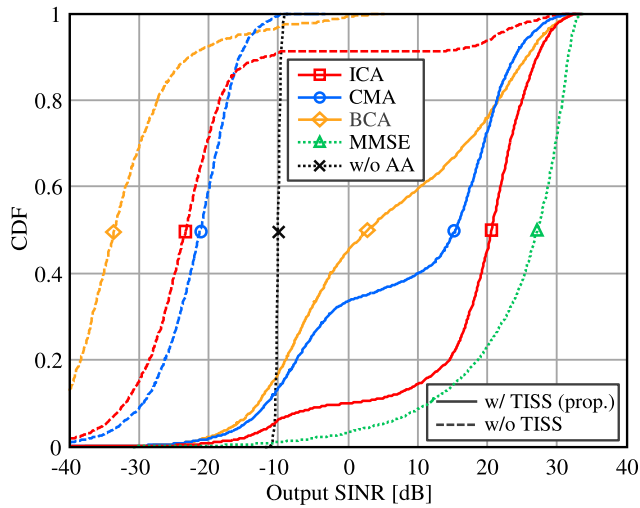
FIGURE 6. CDFs of array output SINR ($N_t = 2$, $N_r = 2$, 16QAM, $N_s = 100$, SIR = −10 dB).

FIGURE 7. Array output SINR with iteration step ($N_t = 2$, $N_r = 2$, 16QAM, $N_s = 100$, SIR = −10 dB).

principle for BCA is geometrical inherence, i.e. *convex perimeter*, on IQ two-dimensional plane. It also requires the condition that is *compactness*. Application of TISS is considered to satisfy it because the QAM symbol arrangement of the desired signal is well visible in that of the Gaussianized interference signal. Convex perimeter is also focused on the amplitude domain similar to that of CMA, so that its interference suppression performance strongly depends on the power ratio to the desired signal. Such an indicator for QAM signals seems to be weak for TISS against the Gaussian distribution. It is not applicable to suppress a large level of interference. The main focus of our proposal, i.e. the kurtosis for ICA and the constancy for CMA, can be obviously differentiated with that for the Gaussian distribution. Especially for ICA, it attained satisfactorily improved interference suppression capability even in such an interference-dominated situation. In this case, the kurtosis of the desired signals is −0.68 whereas that for Gaussianized interference is around −0.01 as shown in Fig. 5. Suppose the required output SINR is 10 dB, ICA can satisfy it for 85.6%. CMA can also exhibit good output SINR in 60.1% even in the use of multi modulus 16QAM signals. The remaining percentiles should be improved further; BAAs have not reached the convergence. It would depend on the spatial correlation among the desired/interference signals. Other physical layer signal processing, e.g. forward error correction, can compensate for such a room for improvement. As for the MMSE, the number of pilot symbols is set to be the same as that of receiving antenna elements and these sequences are orthogonal among users. Although it should exhibit the best SINR performance thanks to a priori information, its overhead is inevitable. Practically, the number of pilot signals is limited and hence its sequence should be rigorously designed so as to keep the (quasi-)orthogonality. The proposed concept is also supportive of alleviating such limitations.

Fig. 7 shows the convergence characteristics with the iteration count for each BAAs in the cases of 16QAM, $N_s = 100$,
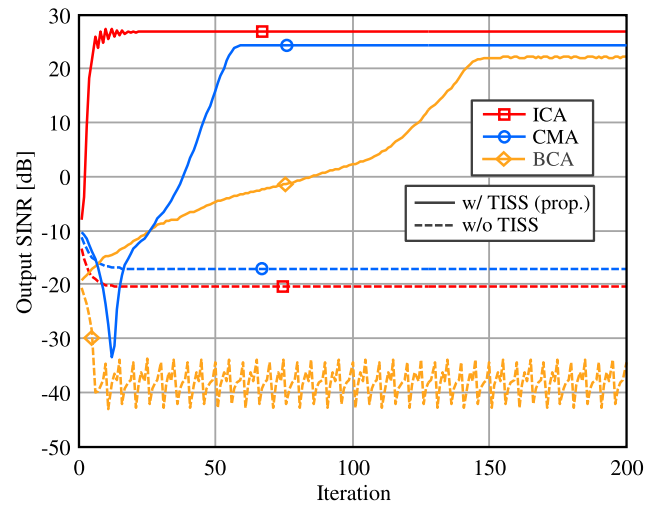
and input SIR = −10 dB. The figure exemplifies the result of the one trial, but they show almost the consistent tendency. In conventional BAAs, capturing the interference signal as large as 10 dB leads to convergence in a few iterations since their optimization criteria can be easily satisfied. Although ICA and CMA with TISS require slightly more iterations than the conventional schemes to converge, they can successfully attain good output SINR larger than 10 dB. From the case study shown in Fig. 7, it is about 10 iterations for ICA and about 60 for CMA; 100 iterations are sufficient. BCA with TISS requires more iteration to the optimal; its maximum count is set to 200. We can observe the above tendency generally holds; ICA converges faster and achieves higher output SINR than CMA.

Following evaluations focus on the median value of the array output SINR distribution. Fig. 8 shows the median value of array output SINR obtained by ICA and CMA with input SIR. This case also employs 16QAM and $N_s = 100$. The figure plots the characteristics without BAA processing as a reference in which input and output values almost correspond. Conventional schemes without TISS can obtain sufficient output SINR at SIR > 0 dB whereas they cannot work at the opposite condition where SIR < 0 dB. It implies that the original BAA algorithms capture the signal having larger power and suppress the other one having lower power. The proposed scheme, ICA with TISS, can achieve consistent output SINR over 20 dB irrespective of the interference level. Even in the case of CMA with TISS, a significant output SINR can be achieved when the input SIR is larger than −10 dB. CMA can also be sufficiently applicable depending on the requirement, such as target SINR, the signal processing capability, and the processing delay related to the iteration. In other words, when TISS is applied, the desired signal can always be obtained while using ICA or CMA without any additional control such as the interference level estimation and the algorithm switching referring to its estimation result. Regarding BCA, although the array output is improved,
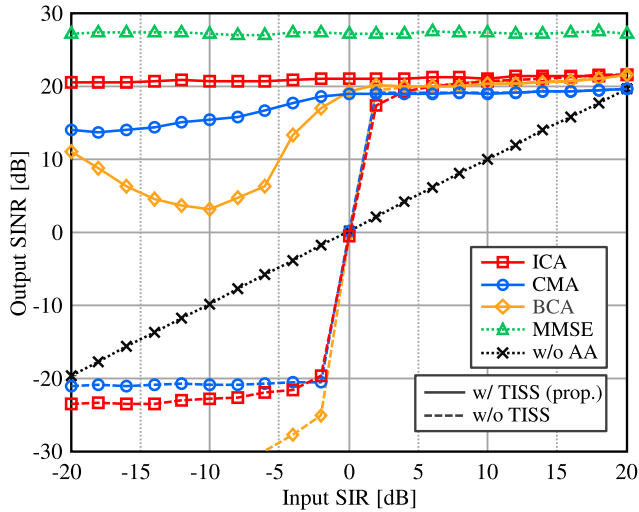
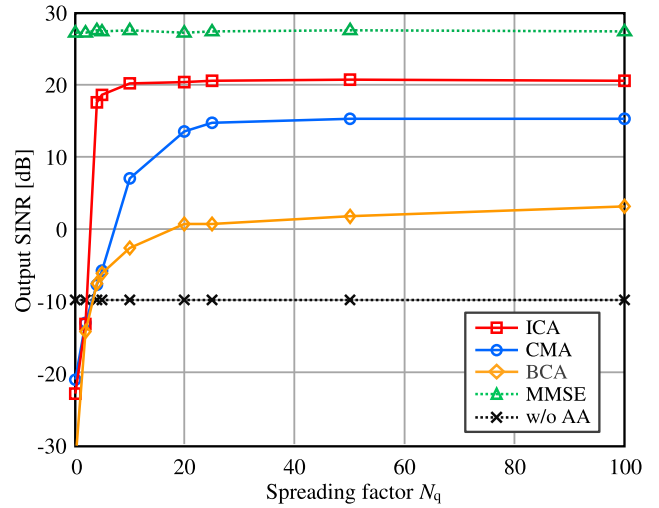**FIGURE 8.** Median value of array output SINR with input SIR ($N_t = 2$, $N_r = 2$, 16QAM, $N_s = 100$).

FIGURE 10. Median value of array output SINR with spreading factor ($N_t = 2$, $N_r = 2$, 16QAM, $N_s = 100$, SIR $= -10$ dB, w/TISS).
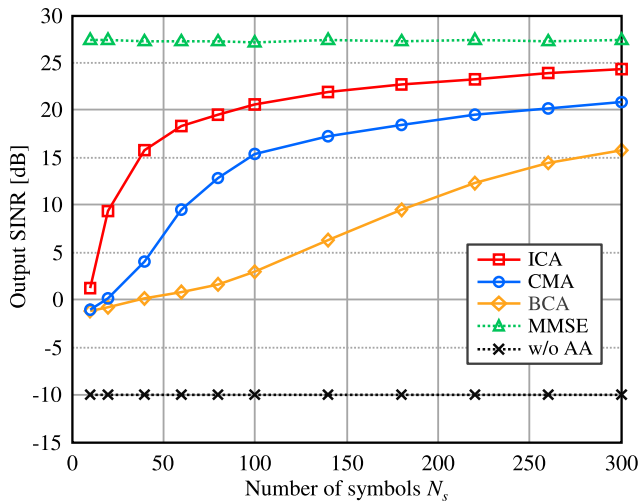

FIGURE 9. Median value of array output SINR with symbol amount ($N_t = 2$, $N_r = 2$, 16QAM, SIR $= -10$ dB, w/TISS).

FIGURE 11. Median value of array output SINR with modulation order ($N_t = 2$, $N_r = 2$, $N_s = 100$, SIR $= -10$ dB, w/TISS).

it has not reached a level that can withstand practical use.

Under the application of TISS, Fig. 9 shows the median value of array output SINR with the number of symbols N_s at the input SIR $= -10$ dB. Array output SINR by ICA-TISS tends to be saturated at around 200 symbols. The size of the spreading matrix $\mathbf{Q}_i$ is defined as the same as the symbol amount N_s. As the number of symbols increases, statistics of the interference signal approaches the normal distribution, so that the identification accuracy could be improved. Furthermore, output SINR $= 15$ dB or more can be attained at 50 symbols. ICA-TISS can provide good interference suppression capability even with the reduced number of symbols. Especially in the smaller symbol amount region, the superiority of ICA over CMA can be confirmed.

Performance dependency on the spreading factor is then examined. Fig. 10 plots median values of array output SINR with the spreading matrix size, N_q. Fix the symbol amount to
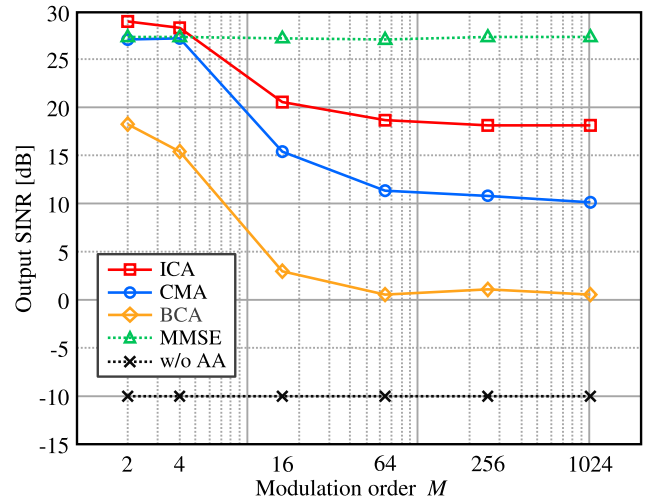
$N_s = 100$, other parameters are set to $N_t = N_r = 2$ and input SIR $= -10$ dB. Increasing N_q surely improves interference suppression performance for all BAA algorithms. $N_q = 10$ is sufficient for ICA while 20 or more is required for CMA and BCA. Statistical inherence such as peakedness and tailedness comprising kurtosis can be extracted with comparative ease, whereas the amplitude-based metrics such as constancy and convex perimeter require more strict Gaussianization to recognize the desired signal.

Finally, the median value characteristics of array output SINR with modulation order is disclosed in Fig. 11. In this case, the input SIR $= -10$ dB and $N_s = 100$. Interference suppression performance tends to be degraded as the modulation order, M, increases. It is because the kurtosis gets larger and the number of signal envelopes are increased with M as expressed in (15) and (16), respectively. It should be noted that the degradation for ICA is converged in 256QAM or
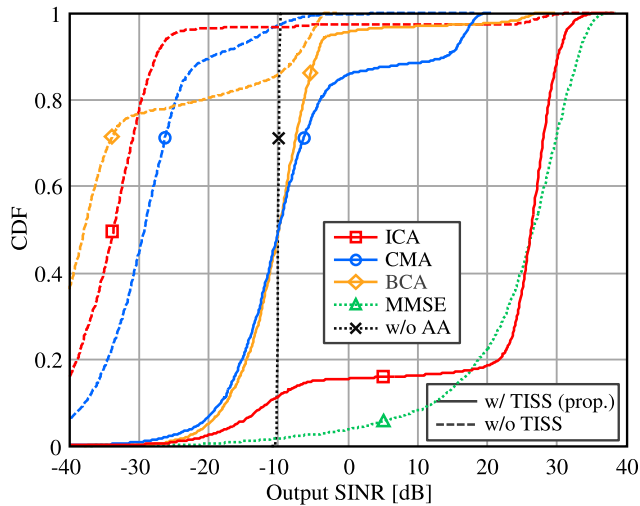
FIGURE 12. CDFs of array output SINR ($N_t = 4$, $N_r = 16$, 16QAM, $N_s = 800$, SIR = −10 dB).

FIGURE 13. Array output SINR with iteration step ($N_t = 4$, $N_r = 16$, 16QAM, $N_s = 300$, SIR = −10 dB).

FIGURE 14. Median value of array output SINR with input SIR ($N_t = 4$, $N_r = 16$, 16QAM, $N_s = 300$).

higher since their original kurtosis values are around −0.60. ICA can keep good output SINR median value around 20 dB even in 1024QAM; the desired and interference signals are distinguishable thanks to the TISS operation which modifies the kurtosis value to almost zero. It indicates that such a higher modulation order is fully applicable when SNR is higher or array antenna gain is available. Although the effectiveness of CMA can also be observed, its achievable output SINR is limited compared to the ICA. An increase in the signal envelope number largely affects the signal separation capability for the constant modulus criterion. Unfortunately, the overall performance of BCA is inferior to the other candidates in terms of symbol amounts and modulation order.

C. RESULTS: 4 × 16 CASE
In the next case, we set $N_t = 4$ transmitters and $N_r = 16$ receiver antenna elements to assess the impact of more interference sources and excessive degree of freedom at the receiver side. Fig. 12 shows CDFs of array output SINR in the case with 16QAM, $N_s = 800$, input SIR = −10 dB. Effectiveness of ICA is kept and it shows a significant improvement exceeding the 10 dB output SINR in about 85% range. It is nearly approaching the optimal MMSE performance. On the other hand, the improvement of CMA is limited. The increase of spread interference sources hinders the capturing capability of the desired signal. CDF of BCA also exhibits a similar tendency. As mentioned above, amplitude-based optimization criteria are strongly constrained by the number of signal sources.

To observe the above characteristics in detail, the transition of the output SINR with the iteration count is plotted in Fig. 13. Same as the case of 2 × 2, the desired signal is suppressed and exhibits unusefully low output SINR without TISS. Although the application of TISS is effective, both the improvement of convergence and output SINR are getting
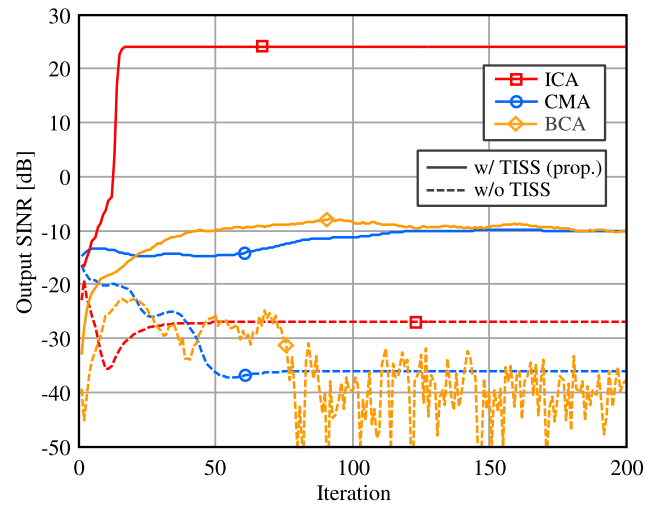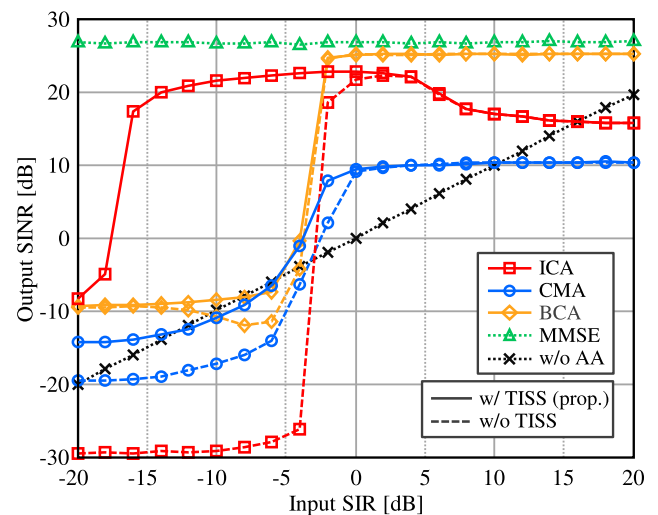
dull except for ICA. Due to the increase in the number of signal sources that produce multiple local optima, CMA and BCA struggle to derive the optimal weight to extract the desired signal even under the application of the proposed TISS. On the other hand, it can be seen that ICA is able to derive the optimal solution with reasonable iterations and suppress interference even under such a severe condition. This is because CMA and BCA focus only on the amplitude domain, that is, the tailedness on the IQ plane, while ICA considers the higher-order statistics representing the form of a probability distribution, i.e. the peakedness as well as tailedness as indices of optimization.

Fig. 14 shows the median value of the array output SINR for the input SIR. This case shows the number of symbols at $N_s = 300$. Input SIR value to invert output SINR (for BAAs without TISS) is shifted to the minus region. It is because the interference power is measured as the sum of
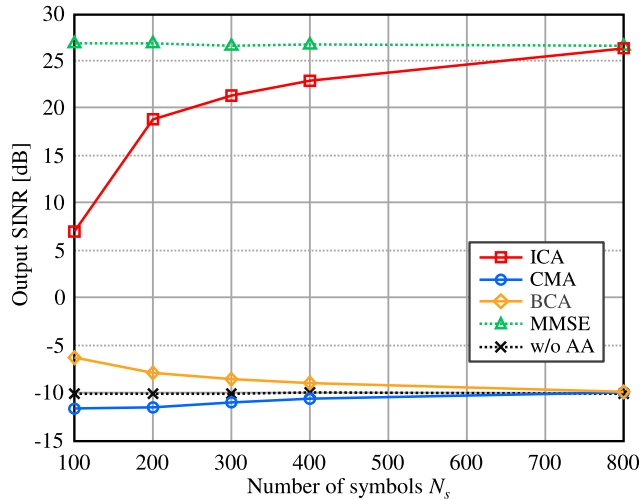
FIGURE 15. Median value of array output SINR with symbol amount ($N_t = 4$, $N_r = 16$, 16QAM, SIR $= -10$ dB, w/TISS).

FIGURE 16. Median value of array output SINR with modulation order ($N_t = 4$, $N_r = 16$, $N_s = 300$, SIR $= -10$ dB, w/TISS).

TABLE 3. Computation complexity.

	Complexity order	CPU running time [sec]	
		$N_r = 2$	$N_r = 16$
ICA	$\mathcal{O}(N_k N_m N_r N_s)$	0.7416	0.7507
CMA	$\mathcal{O}(N_m N_r N_s)$	0.0012	0.0024
BCA	$\mathcal{O}(N_m N_s (N_r + \log N_s))$	0.0043	0.0067

CPU running time is examined with 16QAM, $N_s = 100$, $N_m = 100$, $N_k = 2497$.

that from the other three transmitters. ICA-TISS can achieve good output SINR more than 20 dB at $-14 \leq$ SIR ≤ 4 dB whereas at SIR > 4 dB, it tends to be degraded despite the sufficiently high desired signal power. An excessively large number of receiving antennas, i.e. observation points, also may deliver array weights to the local optimal solution. It also be because the interference signal level is small and close to the noise; caused an imperfect interference cancellation. Figs. 15 and 16 show the median array output SINR with the number of symbols, N_s, and the modulation order, M, when the input SIR is -10 dB and TISS is applied. ICA-TISS shows reasonable SINR with 200 symbols or more while there is no negative dependence on higher modulation order. Except for this condition on ICA-TISS, none of the other BAA algorithms are able to achieve sufficient interference suppression performances. We can conclude that the ICA based on the non-amplitude based optimization principle can achieve excellent blind interference suppression performance in various environments under the application of TISS.

D. COMPUTATION COMPLEXITY

Here we discuss computation complexity which is defined as the number of multiplications. In ICA, calculation of kurtosis and the residual error is dominated by the matrix-vector product such as $\mathbf{X}\mathbf{y}^H$, which requires $N_r N_s$ multiplications. In addition, ICA requires search process for the optimal step size, μ_{opt} among N_k candidates, and the iterative process for the weight update with N_m times. Computation order for ICA becomes $\mathcal{O}(N_k N_m N_r N_s)$. Although CMA contains the matrix-matrix product as $(\mathbf{XX})^{-1}\mathbf{X}\mathbf{e}_{\text{CMA}}$, $(\mathbf{XX})^{-1}\mathbf{X}$ part is invariant against the iterative process. It is sufficient to calculate once beforehand, and hence the dominant computation becomes $N_r N_s$. With considering the N_m iteration, complexity order of CMA can be estimated as $\mathcal{O}(N_m N_r N_s)$. As for BCA, the most dominant operation is the extraction
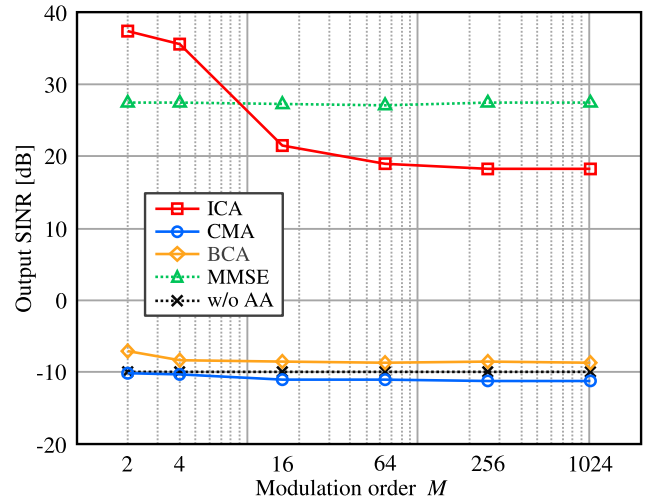
of the convex hull from the N_s points, which is known to be $\mathcal{O}(N_s \log N_s)$ [29]. It should be repeated for N_m, so that the overall complexity order is $\mathcal{O}(N_m N_s (N_r + \log N_s))$. Note that BCA also contains weight application $\mathbf{y} = \mathbf{w}_{\text{BCA}}^H(m)\mathbf{X}$ which requires $N_r N_s$ multiplications in the iteration process same as the other algorithms. ICA has an extensive computational load due to a double optimization process whereas it can provide outstanding interference suppression performance in combination with the proposed TISS.

Table 3 summarizes complexity order and CPU running time for BAA weight calculation. Running time is examined by using Intel(R) Core(TM) i9-10980XE CPU and is averaged over 3,000 trials. Representative parameters are the iteration count $N_m = 100$ and the number of symbols $N_s = 100$, respectively. For ICA, the number of step size candidates, N_k, is 2497. We can confirm that the relationship among the computation time for BAA algorithms almost agrees with the estimated order based on multiplications. CMA exhibits the fastest computation even though it contains the computation of $(\mathbf{XX})^{-1}\mathbf{X}$. The computation time for ICA is larger than the others because it requires an optimal step size search in (9). It will be shortened by devising hardware implementation such as parallel processing. In this study, the step size is approximately thoroughly searched for reliable weight derivation, but its simplification is an issue to be addressed for feasibility verification.

The proposed TISS requires additional computation to generate the spreading matrix, $\mathbf{Q}$. The complexity order for its preparation is known to $\mathcal{O}(N_q^3)$ for the QR decomposition [46, p 249], or less for the matrix inversion [47, p. 12], [48]. Sufficient output SINR can be provided with $N_q = 10$ for ICA and around 20 for CMA and hence the computation complexity required for spreading matrix derivation can be practically acceptable, compared with thoroughly preparing the spreading matrix with the size of the number of symbols N_s. Here, $\mathbf{Q}$ could be calculated once preparatory to operation and stored in the internal memory, or updated at regular interval. It is possible to substantially avoid the computational impact on practical use.

E. DISCUSSION

The above evaluation exhibited the fundamental effectiveness of the proposed scheme suppressing the interference signal even when its power is larger than that of the desired signal. The following discussion throws related issues and future challenges for the proposed approach.

We considered the simple line-of-sight channel model with the narrow band single-carrier transmission in order to strictly evaluate the BAA interference suppression performance under the deterministic SIR condition. Results clarified that the proposed scheme does work irrespective of SIR and hence it could be applicable for Rayleigh fading channel environment where signal strengths, i.e. SIR, fluctuate instantly. Its practical application is OFDM transmission. In this case, the proposed scheme can be simply extended by applying per subcarrier. Blind interference suppression capability based on OFDM should be verified through a link level evaluation, under the general wideband channel environment with multipath fading. Meanwhile, in an asynchronous transmission case, a possibility of eased signal separation was suggested in [33]. Sampling timing deviation decreases the kurtosis of the interference signal, i.e. distribution goes to the Gaussian. Its realistic impact is an interesting issue to be studied as an extension of our proposed concept.

As a concrete application example, the proposed scheme could be effective for uplink interference cancellation in a multicell environment [49], [50] where inter-cell CSI is unavailable. The spreading matrix can be regarded as unique words that can contribute to separate signal sources. Preparing respective spreading matrices for each transmitter is expected to successfully extract the desired signals without the use of CSI. It is expected contributing to resolving the *pilot contamination* problem [51]. This promising nature would be able to realize a perfect blind MIMO without any identification overhead. The blind MIMO well investigated so far necessitates identifying which antenna they were transmitted from after ICA signal source separation [20], [21]. It can be realized by detecting the desired signal stream that matches the unique word after BSS. However, the receiver needs to know how many signals are impinging. This approach is unavailable for such as CMA; it extracts only the

signal having the highest amplitude, so there is no means to obtain the other signals. The proposed scheme by TISS can extract the desired signal regardless of the signal level or the strength of the properties of the signal. The spreading matrix itself has the identification function; it can be understood as a kind of a priori information.

As for the issues behind the proposed approach, the impact on the orthogonality among the time-domain symbols should be considered. Time varying channels, brought by the mobility of user terminals, may break the orthogonality among spread symbols. The original signal sequence cannot be obtained even after the de-spreading operation. The BAA algorithms require several data symbols and hence the above impact on the mobility environment should also be further investigated while exploring enhancement approaches.

VI. CONCLUSION

This paper newly proposed the interference Gaussianization scheme by time-domain symbol spreading which can expand the operational region of the blind adaptive array signal source identification in terms of the input SIR. The transmitter applies a spreading matrix to the desired transmission signal and the receiver de-spreads the mixture of the desired and interference signals, using the preshared same matrix. It results in spreading only interference components so as to have the Gaussian distribution, i.e. intentionally reduces the kurtosis for ICA and breaks the constant envelope property for CMA. It leads both ICA and CMA to well capture the desired signal and hence these weight optimization criteria appropriately and efficiently work to suppress the interference signals. Computer simulation verified its fundamental effectiveness; ICA and CMA with TISS successfully realized interference suppression at the region SIR < 0 dB where was out of the range conventionally, even in the use of higher modulation order. Although the effectiveness of CMA-TISS is limited to a few numbers of signal sources, ICA-TISS presents wide capability for a larger number of not only sources but also receiver antenna elements. If we carefully chose the application situation for CMA-TISS, it is still useful under the use of specified parameters such as symbol amounts and the modulation order. The proposed approach has a promising possibility to resolve various co-channel interference problems.

REFERENCES

[1] X. Gelabert, P. Legg, and C. Qvarfordt, "Small cell densification requirements in high capacity future cellular networks," in *Proc. IEEE Int. Conf. Commun. Workshops (ICC)*, Jun. 2013, pp. 1112–1116.

[2] X. Ge, S. Tu, G. Mao, C. X. Wang, and T. Han, "5G ultra-dense cellular networks," *IEEE Wireless Commun.*, vol. 23, no. 1, pp. 72–79, Feb. 2016.

[3] J. Mitola and G. Q. Maguire, "Cognitive radio: Making software radios more personal," *IEEE Pers. Commun.*, vol. 6, no. 4, pp. 13–18, Aug. 1999.

[4] S. Haykin, "Cognitive radio: Brain-empowered wireless communications," *IEEE J. Sel. Areas Commun.*, vol. 23, no. 2, pp. 201–220, Feb. 2005.

[5] H. Li, Y. Yang, Y. Dou, J. J. Park, and K. Ren, "PeDSS: Privacy enhanced and database-driven dynamic spectrum sharing," in *Proc. INFOCOM IEEE Conf. Comput. Commun.*, Apr. 2019, pp. 1477–1485.

[6] W. S. H. M. W. Ahmad, N. A. M. Radzi, F. S. Samidi, A. Ismail, F. Abdullah, M. Z. Jamaludin, and M. N. Zakaria, "5G technology: Towards dynamic spectrum sharing using cognitive radio networks," *IEEE Access*, vol. 8, pp. 14460–14488, Jan. 2020.

[7] K. Sato and T. Fujii, "Kriging-based interference power constraint: Integrated design of the radio environment map and transmission power," *IEEE Trans. Cognit. Commun. Netw.*, vol. 3, no. 1, pp. 13–25, Mar. 2017.

[8] Y. Jian, C.-F. Shih, B. Krishnaswamy, and R. Sivakumar, "Coexistence of Wi-Fi and LAA-LTE: Experimental evaluation, analysis and insights," in *Proc. IEEE Int. Conf. Commun. Workshop (ICCW)*, Jun. 2015, pp. 2325–2331.

[9] N. Patriciello, S. Lagén, and B. Bojović, "NR-U and IEEE 802.11 technologies coexistence in unlicensed mmWave spectrum: Models and evaluation," *IEEE Access*, vol. 8, pp. 71254–71271, Apr. 2020.

[10] G. Naik, J.-M. Park, J. Ashdown, and W. Lehr, "Next generation Wi-Fi and 5G NR-U in the 6 GHz bands: Opportunities and challenges," *IEEE Access*, vol. 8, pp. 153027–153056, Aug. 2020.

[11] K. Maruta, J. Mashino, and T. Sugiyama, "Blind adaptive arrays with subcarrier transmission power assignment for spectrum superposing," in *Proc. Asia–Pacific Microw. Conf.*, Nov. 2014, pp. 567–569.

[12] K. Maruta, J. Mashino, and T. Sugiyama, "Blind interference suppression scheme by eigenvector beamspace CMA adaptive array with subcarrier transmission power assignment for spectrum superposing," *IEICE Trans. Commun.*, vol. E98.B, no. 6, pp. 1050–1057, 2015.

[13] T. Tabata, H. Asato, D. Hai Pham, M. Fujimoto, N. Kikuma, S. Hori, and T. Wada, "Experimental study of adaptive array antenna system for ISDB-T high speed mobile reception," in *Proc. IEEE Antennas Propag. Soc. Int. Symp.*, Jun. 2007, pp. 1697–1700.

[14] R. T. Compton, "The power-inversion adaptive array: Concept and performance," *IEEE Trans. Aerosp. Electron. Syst.*, vol. AES-15, no. 6, pp. 803–814, Nov. 1979.

[15] K. Nishimori, N. Kikuma, and N. Inagaki, "The differential CMA adaptive array antenna using an Eigen-beamspace system," *IEICE Trans. Commun.*, vol. 78, no. 11, pp. 1480–1488, Nov. 1995.

[16] J. Treichler and B. Agee, "A new approach to multipath correction of constant modulus signals," *IEEE Trans. Acoust., Speech, Signal Process.*, vol. ASSP-31, no. 2, pp. 459–472, Apr. 1983.

[17] B. Agee, "The least-squares CMA: A new technique for rapid correction of constant modulus signals," in *Proc. IEEE Int. Conf. Acoust., Speech, Signal Process. (ICASSP)*, Apr. 1986, pp. 953–956.

[18] A. Hyvärinen and E. Oja, "Independent component analysis: Algorithms and applications," *Neural Netw.*, vol. 13, nos. 4–5, pp. 411–430, Jun. 2000.

[19] V. Zarzoso and P. Comon, "Robust independent component analysis by iterative maximization of the kurtosis contrast with algebraic optimal step size," *IEEE Trans. Neural Netw.*, vol. 21, no. 2, pp. 248–261, Feb. 2010.

[20] D. Obradovic, N. Madhu, A. Szabo, and C. S. Wong, "Independent component analysis for semi-blind signal separation in MIMO mobile frequency selective communication channels," in *Proc. IEEE Int. Joint Conf. Neural Netw.*, vol. 1, Jul. 2004, pp. 53–58.

[21] S. R. Curnew and J. Ilow, "Blind signal separation in MIMO OFDM systems using ICA and fractional sampling," in *Proc. Int. Symp. Signals, Syst. Electron.*, Jul. 2007, pp. 67–70.

[22] K. Sugai, H. Yamada, and Y. Yamaguchi, "Fundamental study on blind MIMO transmission by using ICA," in *Proc. Int. Symp. Antennas Propag. (ISAP)*, Oct. 2009, pp. 153–156.

[23] K. Maruta, K. Nishimori, and C.-J. Ahn, "Constant modulus and kurtosis based blind adaptive array interference suppression: Comparisons and new approach," in *Proc. 18th Int. Symp. Commun. Inf. Technol. (ISCIT)*, Sep. 2018, pp. 43–47.

[24] Z. Luo, C. Li, and L. Zhu, "A comprehensive survey on blind source separation for wireless adaptive processing: Principles, perspectives, challenges and new research directions," *IEEE Access*, vol. 6, pp. 66685–66708, 2018.

[25] R. Gribonval and S. Lesage, "A survey of sparse component analysis for blind source separation: Principles, perspectives, and new challenges," in *Proc. 14th Eur. Symp. Artif. Neural Netw.*, Apr. 2006, pp. 323–330.

[26] S. Uehashi, Y. Ogawa, T. Nishimura, and T. Ohgane, "Prediction of time-varying multi-user MIMO channels based on DOA estimation using compressed sensing," *IEEE Trans. Veh. Technol.*, vol. 68, no. 1, pp. 565–577, Jan. 2019.

[27] K. Goto, K. Maruta, and C.-J. Ahn, "Compressed sensing based low complexity 2D-DOA estimation by separation and pair-matching approach," *IEICE Commun. Exp.*, vol. 9, no. 6, pp. 224–229, 2020.

[28] J. Bobin, J. Rapin, A. Larue, and J.-L. Starck, "Sparsity and adaptivity for the blind separation of partially correlated sources," *IEEE Trans. Signal Process.*, vol. 63, no. 5, pp. 1199–1213, Mar. 2015.

[29] S. Cruces, "Bounded component analysis of linear mixtures: A criterion of minimum convex perimeter," *IEEE Trans. Signal Process.*, vol. 58, no. 4, pp. 2141–2154, Apr. 2010.

[30] A. T. Erdogan, "A class of bounded component analysis algorithms for the separation of both independent and dependent sources," *IEEE Trans. Signal Process.*, vol. 61, no. 22, pp. 5730–5743, Nov. 2013.

[31] K. Maruta, S. Kojima, C.-J. Ahn, D. Hisano, and Y. Nakayama, "Blind SIR estimation by convolutional neural network using visualized IQ constellation," in *Proc. IEEE 91st Veh. Technol. Conf. (VTC-Spring)*, May 2020, pp. 1–2.

[32] K.-K. Wong, R. D. Murch, and K. B. Letaief, "Performance enhancement of multiuser MIMO wireless communication systems," *IEEE Trans. Commun.*, vol. 50, no. 12, pp. 1960–1970, Dec. 2002.

[33] H. Mathis, "On the kurtosis of digitally modulated signals with timing offsets," in *Proc. IEEE 3rd Workshop Signal Process. Adv. Wireless Commun. (SPAWC) Workshop*, Mar. 2001, pp. 86–89.

[34] P. H. Westfall, "Kurtosis as peakedness, 1905–2014. *RIP*," *Amer. Statistician*, vol. 68, no. 3, pp. 191–195, Aug. 2014.

[35] S. Denno and T. Ohira, "Modified constant modulus algorithm for digital signal processing adaptive antennas with microwave analog beamforming," *IEEE Trans. Antennas Propag.*, vol. 50, no. 6, pp. 850–857, Jun. 2002.

[36] B. Widrow, P. E. Mantey, L. J. Griffiths, and B. B. Goode, "Adaptive antenna systems," *Proc. IEEE*, vol. 55, no. 12, pp. 2143–2159, Dec. 1967.

[37] N. Kikuma, K. Takai, K. Nishimori, F. Saito, and N. Inagaki, "Consideration on performance of the CMA adaptive array antenna for 16 QAM signals," in *Proc. 6th Int. Symp. Pers., Indoor Mobile Radio Commun.*, vol. 2, 1995, pp. 677–681.

[38] D. S. Lemons, *An Introduction to Stochastic Processes in Physics*. Baltimore, MD, USA: The Johns Hopkins Univ. Press, 2002.

[39] A. Hyvärinen, J. Karhunen, and E. Oja, *Independent Component Analysis*. Hoboken, NJ, USA: Wiley, 2001.

[40] M. Huzak, "Characteristic functions," in *International Encyclopedia of Statistical Science*, M. Lovric, Ed. Berlin, Germany: Springer, 2011, pp. 238–239.

[41] B. Suard, A. F. Naguib, G. Xu, and A. Paulraj, "Performance of CDMA mobile communication systems using antenna arrays," in *Proc. IEEE Int. Conf. Acoust. Speech Signal Process.*, vol. 4, Apr. 1993, pp. 153–156.

[42] B. Xu and T. B. Vu, "Blind MAI and CCI suppression using adaptive array antennas in DS/CDMA mobile communications systems," in *Proc. 4th Int. Conf. Signal Process. (ICSP)*, Oct. 1998, pp. 365–368.

[43] M. Hefnawi and G. Y. Delisle, "Impact of wideband CDMA signals on smart antenna systems," in *Proc. IEEE Int. Conf. Pers. Wireless Commun. Conf.*, Dec. 2000, pp. 5–8.

[44] R. Roy and T. Kailath, "ESPRIT-estimation of signal parameters via rotational invariance techniques," *IEEE Trans. Acoust., Speech, Signal Process.*, vol. 37, no. 7, pp. 984–995, Jul. 1989.

[45] L. Liu and H. Liu, "Joint estimation of DOA and TDOA of multiple reflections in mobile communications," *IEEE Access*, vol. 4, pp. 3815–3823, 2016.

[46] G. H. Golub and C. F. Van Loan, *Matrix Computations*, 4th ed. Baltimore, MD, USA: The Johns Hopkins Univ. Press, 2013.

[47] R. W. Farebrother, *Linear Least Squares Computations*. New York, NY, USA: Marcel Dekker, 1988.

[48] D. Zhu, B. Li, and P. Liang, "On the matrix inversion approximation based on Neumann series in massive MIMO systems," in *Proc. IEEE Int. Conf. Commun. (ICC)*, Jun. 2015, pp. 1763–1769.

[49] K. Maruta and C.-J. Ahn, "Uplink interference suppression by semi-blind adaptive array with decision feedback channel estimation on multicell massive MIMO systems," *IEEE Trans. Commun.*, vol. 66, no. 12, pp. 6123–6134, Dec. 2018.

[50] K. Maruta and C.-J. Ahn, "Improving semi-blind uplink interference suppression on multicell massive MIMO systems: A beamspace approach," *IEICE Trans. Commun.*, vol. E102-B, no. 8, pp. 1503–1511, Aug. 2019.

[51] T. L. Marzetta, "Noncooperative cellular wireless with unlimited numbers of base station antennas," *IEEE Trans. Wireless Commun.*, vol. 9, no. 11, pp. 3590–3600, Nov. 2010.
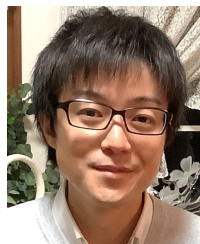
KAZUKI MARUTA (Member, IEEE) received the B.E., M.E., and Ph.D. degrees in engineering from Kyushu University, Japan, in 2006, 2008, and 2016, respectively. From 2008 to 2017, he was with the NTT Access Network Service Systems Laboratories and engaged in the research and development of interference compensation techniques for future wireless communication systems. From 2017 to 2020, he was an Assistant Professor with the Graduate School of Engineering, Chiba University. He is currently a specially appointed Associate Professor with the Academy for Super Smart Society, Tokyo Institute of Technology. His research interests include MIMO, adaptive array signal processing, channel estimation, medium access control protocols, and moving networks. He is a member of The Institute of Electronics, Information and Communication Engineers (IEICE). He received the IEICE Young Researcher's Award, in 2012; the IEICE Radio Communication Systems (RCS) Active Researcher Award, in 2014; the APMC 2014 Prize; the IEICE RCS Outstanding Researcher Award, in 2018; and the IEEE ICCE Excellent Paper Award, in 2021. He was a co-recipient of the IEICE Best Paper Award, in 2018, the SoftCOM 2018 Best Paper Award, and the APCC 2019 Best Paper Award.

KATSUYA SENOO (Graduate Student Member, IEEE) received the B.E. degree in engineering from Chiba University, Japan, in 2018. He joined NTT DOCOMO, in 2020. His research interest includes adaptive array signal processing for spectrum superposing.

DAISUKE HISANO (Member, IEEE) received the B.E. and M.E. degrees in electrical, electronic and information engineering from Osaka University, Osaka, Japan, in 2012 and 2014, respectively.

In 2014, he joined the NTT Access Network Service Systems Laboratories, Yokosuka, Japan. Since October 2018, he has been an Assistant Professor with the Graduate School of Engineering, Osaka University. His research interests include optical-wireless converged networks, optical communication, and all-optical signal processing. He is a member of IEICE.

YU NAKAYAMA (Member, IEEE) received the B.A., M.E., and Ph.D. degrees in agriculture, environmental studies, and information and communication engineering from The University of Tokyo, Tokyo, Japan, in 2006, 2008, and 2018, respectively.

In 2008, he joined the NTT Access Network Service Systems Laboratories, NTT Corporation. He is currently an Associate Professor with the Institute of Engineering, Tokyo University of Agriculture and Technology. He is also the President of the neko 9 Laboratories, which is a nonprofit organization in Tokyo. His research interests include adaptive networks, network architecture, packet switching, and sensor networks. He is a member of IEICE and IPSJ.

KENTARO NISHIMORI (Member, IEEE) received the B.E., M.E., and Ph.D. degrees in electrical and computer engineering from the Nagoya Institute of Technology, Nagoya, Japan, in 1994, 1996, and 2003, respectively. In 1996, he joined the NTT Wireless Systems Laboratories, Nippon Telegraph and Telephone Corporation, Tokyo, Japan. He was a Visiting Researcher with Aalborg University, Aalborg, Denmark, from February 2006 to January 2007. Since 2009, he has been an Associate Professor with Niigata University, Niigata, Japan, where he is currently a Research Professor. His main interests include spatial signal processing and massive MIMO systems. He is a member of IEICE. He was a recipient of the Young Engineers Award from the IEICE of Japan, in 2001; the Young Engineer Award from IEEE AP-S Japan Chapter, in 2001; and the IEICE Best Paper Award, in 2010.

• • •